Transitions between smooth and complex stick-slip sliding of surfaces

Delphine Gourdon and Jacob N. Israelachvili
Department of Chemical Engineering, University of California at Santa Barbara, Santa Barbara, California 93106, USA
(Received 24 February 2003; published 11 August 2003)

Shear measurements were performed on mica surfaces with molecularly thin films of squalane ($C_{30}H_{62}$) confined between them. Squalane is a branched hydrocarbon liquid that can be in the liquid, glassy, or liquid-crystalline state under confinement. The friction forces, especially the transitions between smooth and intermittent (e.g., stick-slip) sliding, were measured over a wider range of applied loads (pressures), sliding velocities (shear rates), and temperatures than in previous studies. The results reveal that, depending on the conditions, qualitatively different behavior can arise in the same system. These include both abrupt and continuous transitions, both upper and lower critical transition temperatures, short and very long transient effects, and chaotic, sawtooth, or sinusoidal stick-slip that can slowly decay with time or distance sheared. The differences between these branched and simpler, e.g., spherical, unbranched molecules are compared, as well as with unlubricated (dry) surfaces and macroscopic (geological) systems.

DOI: 10.1103/PhysRevE.68.021602 PACS number(s): 68.15.+e, 62.10.+s, 62.40.+i, 64.70.Nd

I. INTRODUCTION

One of the most important questions regarding the motion of rubbing surfaces is what happens when one of them is pushed at a *constant* driving velocity or force relative to the other. Often, the surfaces themselves do not move at a constant velocity, i.e., ''smoothly,'' but ''intermittently,'' and when this occurs the *measured* friction force is also not constant. As illustrated in Fig. 1, intermittent motion can be regular, as in the case of regular stick-slip, or irregular, when both the amplitude, frequency, and shapes of the ''friction spikes'' can vary in a chaotic or random way.[1] Such phenomena are now recognized as being common and a central issue in many different systems and disciplines [1,2], including tribology (friction), materials science (fracture, failure), geology (seismic motion, earthquakes), the flow of granular materials (avalanches), and the generation of sound (as in the case of a violin), to name a few.

During smooth sliding, the shearing surfaces move (relative to each other) at the same constant interfacial velocity V_i as the driving velocity V. The measured friction force F is also constant and equal to the real (interfacial) friction force F_i acting between the two surfaces at that time. During intermittent motion, the surfaces alternately ''stick,'' when the shear stress builds up, or ''slip,'' when the stress is rapidly released. The measured and real friction forces, F and F_i, are then different at any instant due to the finite inertia, compliance, and relaxation time(s) of the system. When describing intermittent friction, individual stick-slip events are referred to as ''spikes,'' which can have various shapes [3]. Very large ''stiction spikes'' are often encountered at the commencement of motion, which can cause surface damage. In the case of geological movement, a large spike or a bundle of spikes would be referred to as an earthquake. Stick-slip spikes can be regular (periodic), chaotic, or erratic (also referred to as irregular, random, stochastic, or noisy). When subjected to detailed analysis, it is often found that the motion in the smooth-sliding regime is really intermittent—characterized by many microspikes that are ''chaotic'' rather than ''random'' [4] (see inset in Fig. 1).

Much work has already been done on the shearing properties of molecularly thin liquid films—including both ''good'' lubricating fluids such as linear or branched chained hydrocarbons or polymer melts, and simple liquids that are not normally employed as lubricants—using the surface forces apparatus (SFA) [3,5], atomic force microscope (AFM) [6], and related techniques [7]. In addition, extensive molecular-dynamics simulations have set the framework for a much better understanding of the behavior of surfaces and fluids under shear [8]. In the case of certain polymer surfaces [9] and branched chained hydrocarbon liquids, which are commonly used in ''lube oils,'' SFA shear measurements on ''single asperity'' molecularly smooth micron-sized contacts have revealed surprisingly long relaxation times and large characteristic ''memory distances'' [4,10,11]. Significantly, the observed frictional behavior of these ''molecular'' systems was found to be surprisingly similar to those observed with macroscopic multicontact surfaces as well as certain

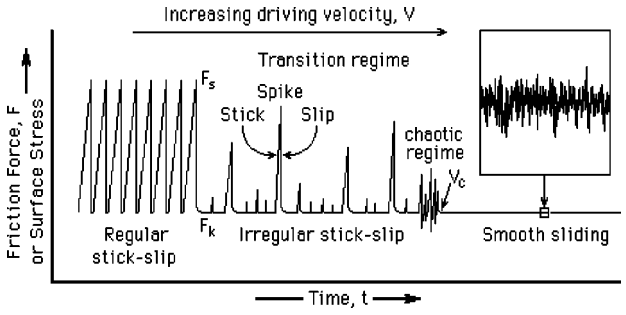

FIG. 1. Smooth and intermittent motion, or the resulting (measured) friction force produced by a *constant* driving force or velocity. Such complex behavior arises because the location where the external force or motion is applied or measured is generally different from the shearing interface where the friction force is generated [3]. Whether the stick-slip is chaotic or random requires a detailed mathematical analysis of the friction traces, recorded over a long period of time [4].

[1]Mathematically, chaotic and random are not synonymous: chaotic motion may appear to be random but is deterministic; random motion is totally unpredictable.

seismic phenomena, albeit over much larger length and time scales. Here we extend our SFA studies over a much larger range of experimental variables, especially to higher loads (pressures) and temperatures, which are closer to those commonly encountered in engineering and seismic systems, and find new and more complex behaviors that have not been seen before *in the same system*.

II. EXPERIMENTAL SECTION

A surface forces apparatus (SFA), when modified for shear studies, allows for two contacting surfaces to be slid past each other at different driving velocities V at the same time as the applied load L and friction forces F are measured. The experiments described in this paper were performed with a new type of SFA, that combines the better features of the two previous versions, and they extend the range of controlled parameters [12,13]. Back-silvered atomically smooth mica surfaces were the primary surfaces used to confine the lubricant films under study. They were glued onto cylindrically curved silica disks, and placed in the sealed SFA with their axes perpendicular to each other, before a droplet of the nonvolatile liquid was injected between them.

To extend the range of the measurements, the following modifications were made in the SFA. (i) The radii of some of the curved silica disks were reduced from 20 mm to 2 mm, allowing for higher contact *pressures* to be attained under a given *load*. The highest (mean) pressures achieved were tens MPa, which may be compared with typical geological pressures occurring at rock junctions. (ii) The piezoelectric bimorph slider [13] was extended, allowing for a larger range of sliding distances to be covered—up to 0.35 mm—before reversing. The driving velocities V available with the ''extended bimorph slider'' ranged from Å/s (stick-slip conditions) to mm/s (smooth sliding conditions).

As in previous SFA experiments, the surfaces were visualized optically with multiple beam interferometry (MBI) using ''fringes of equal chromatic order'' (FECO), that allow the surface shape, contact radius r, area $A=\pi r^2$, and film thickness D to be measured (the latter to an accuracy of 1 Å) either under quiescent conditions or during sliding [14]. An enormous advantage of the direct visualization of the contact region with FECO is that any damage of the surfaces, or undesirable particle or contamination, can be easily and immediately detected (usually accompanied by a change in the friction force). All the friction results reported here were obtained in the ''wearless'' regime, i.e., between undamaged atomically smooth mica surfaces.

The liquid studied, squalane, was provided by Exxon Lube Technology Research Division. Squalane, of chemical formula 2,6,10,15,19,23-hexamethyltetracosane ($C_{30}H_{62}$), is a branched hydrocarbon model lubricant fluid with a viscosity of 6 cP and a refractive index of 1.453 at 26 °C, a melting point of -38 °C, and a boiling point of $+350$ °C. Squalane was chosen because it represents a liquid whose structure lies between simple linear alkanes and ''complex'' branched polymers. It is also used as a model for lubricating oils, and previous studies [4,10,15] have shown it to exhibit a variety of interesting tribological properties.

Prior to injection, the liquid was filtered through a 0.25-μm filter to remove particles. The SFA was purged with dry nitrogen gas for 3 h prior to injecting the liquid between two freshly cleaved and mounted mica surfaces. After injecting a drop of ~ 50 μL, the system was allowed to thermally equilibrate, typically for 2–3 h. During the measurements, a low flow of nitrogen gas was maintained through the SFA chamber to ensure dry conditions throughout the experiment.

For the high-temperature experiments, a UV-setting glue (NOA 61, Norland Products, NJ) was used to mount the mica sheets. This glue, after cross-linking with UV light, remains elastic and rigid at high temperatures, in contrast to the EPON™ glues commonly used in SFA experiments, which become noticeably viscoelastic above 40–50 °C.

III. RESULTS

In all the experiments reported here, the squalane film *at rest* was 1.5–1.7 nm thick, and exhibited a small dilatency when sheared, that increased roughly logarithmically with velocity as found previously [10].

A. Effect of load and sliding velocity on the stick-slip to smooth sliding transition

Figure 2 shows how the measured friction forces F vary with velocity V at different loads L, measured under steady-state conditions, i.e., after the friction traces no longer changed with time. Steady-state conditions were sometimes reached only after several hours of continuous (back and forth) shearing. In general, there was ''regular'' stick-slip at low velocities that disappeared above a certain critical velocity, V_c, above which the sliding was ''smooth.'' This type of behavior is common to systems where the friction force-velocity curve has a negative slope [1], although the details of the transition from stick-slip to smooth sliding at $V=V_c$ can be very different. Here, V_c was largely independent of the load L, but the nature of the transition changed with the load: at low loads and pressures [Figs. 2(a) and 2(b)] the transition was continuous, progressing through an irregular regime characterized by a gradually decreasing stick-slip amplitude $\Delta F=F_s-F_k$ and an increasingly erratic periodicity. This is the same as previously measured by Drummond and Israelachvili [10], who studied the tribology of squalane films at low loads, and who concluded after a detailed mathematical analysis of the stick-slip that it was chaotic rather than random [4]. For such continuous transitions, it is difficult to define a precise value for V_c [see elliptical regions in Figs. 2(a) and 2(b)].

At high loads[2] the transition, shown by the shaded bands in Figs. 2(c) and 2(d), was characterized by a roughly constant stick-slip amplitude ΔF, but with a chaotically increasing *period* or time between the spikes, until the stick-slip

[2]The panels in Fig. 2 also show the mean pressures, defined by $P=L/A$, for each load. However, according to the Hertz theory [16], the pressure is not expected to be uniform throughout the contact circle. Maximum pressure is expected to occur at the center, and to equal $1.5L/A$.

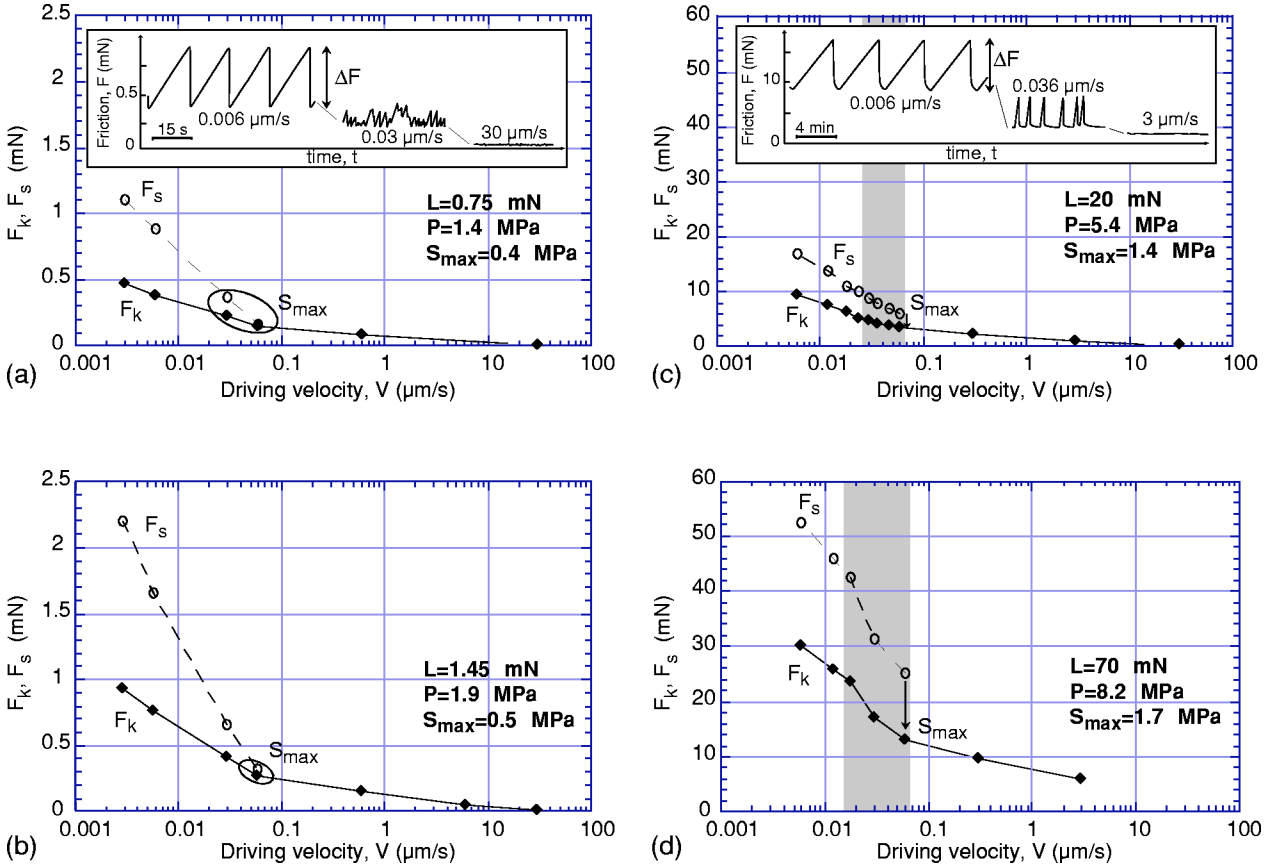

FIG. 2. Steady-state friction forces F vs sliding velocity V at different loads L, all measured at $T=26\,^{\circ}\mathrm{C}$. The stick-slip amplitude is defined by $\Delta F=F_s-F_k$, where by convention F_s and F_k are the static and kinetic friction forces, respectively. At each load L the contact area A remained roughly constant (independent of V) so that the mean pressure $P=L/A$ was also roughly constant. $S_{\max}=F_{\max}/A$ is the maximum shear stress achieved in the smooth sliding regime, i.e., at the transition. Sections taken from real (measured) friction traces are shown in the insets of the upper panel graphs.

disappeared abruptly at a well-defined $V=V_c$ [see vertical arrows in Figs. 2(c) and 2(d)]. This type of discontinuous transition has previously been seen only with spherical and short linear (unbranched) chain molecules that can become well-ordered between two surfaces [17–19].

Once in the smooth sliding regime, the kinetic friction forces continued to decrease with increasing sliding velocity, indicative of continued ''shear thinning.'' It is important to note that, in general, the transition from stick-slip to smooth sliding is believed to require that $dF_i/dV<0$, i.e., that the slope of the intrinsic friction force-velocity curve is negative, as observed here. However, both the functional form of $F_i(V)$ *and* the inertia and compliance of the measuring instrument or ''machine,'' e.g., the stiffness of the friction-force measuring spring, determine the critical velocity V_c and other features of the transition [20].

B. Effect of normal load on the friction force and contact area

Figure 3(a) shows the friction versus load at two sliding velocities in the smooth sliding regime ($V>V_c$). In each case F increases linearly with L, obeying Amonton' first law, viz., that the coefficient of friction, defined by

$$\mu=F/L \tag{1}$$

or[3]

$$\mu=dF/dL \tag{2}$$

is constant. But μ falls with increasing velocity, from $\mu=0.125$ at $V=0.6$ μm/s to $\mu=0.06$ at $V=30$ μm/s, which is contrary to Amontons' second law. Figure 3(a) also shows the contact areas at the different loads. These were independent of the sliding velocity (hence there is only one curve), and appear to be well-described by the Hertz theory for non-adhering contacts (dashed curve), which is given by

$$A=\pi(RL/K)^{2/3}, \tag{3}$$

where R is the initial (undeformed) radius of the surfaces and K is the elastic modulus of the substrate material (in units of Pa). The above analysis shows that the friction force follows Amontons' prediction ($F=\mu L$, $\mu=$const) as the contact area follows the Hertzian prediction ($A\propto L^{2/3}$). In other

[3]In cases where there is a finite friction already at zero load, the friction coefficient is usually defined by Eq. (2). In the case of a straight line passing through the origin, the two definitions, given by Eqs. (1) and (2), are equivalent.

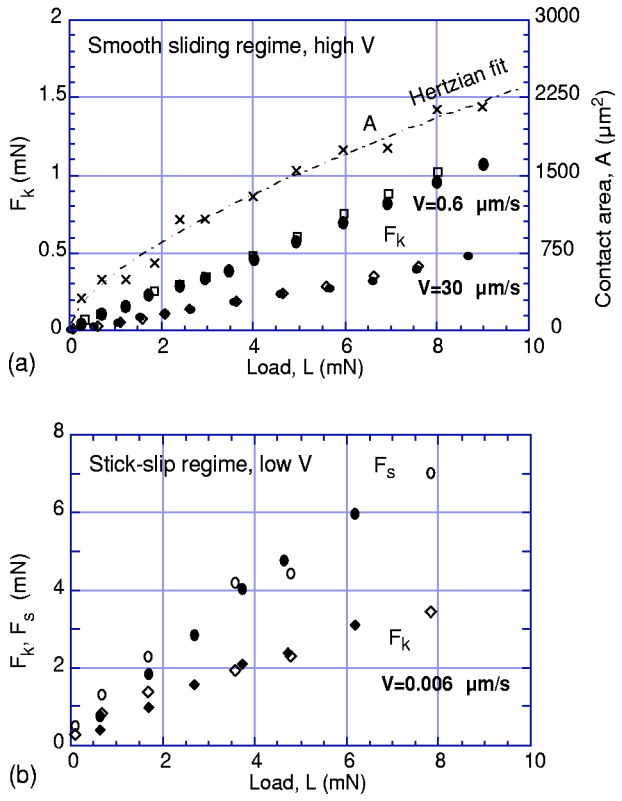

FIG. 3. (a) Steady-state friction forces F (left ordinate) and contact area A (right ordinate) vs normal load L at two different driving velocities V in the smooth-sliding regime, i.e., at $V>V_c$. For the friction forces, black points refer to loading conditions (increasing L), white points to unloading conditions (decreasing L). No "hysteresis" was observed in these measurements. The contact area is shown by crosses, and the dashed line is the Hertzian fit to the area vs load data, Eq. (3), using $K=10\times10^9$ N/m^2. (b) Same as (a) but in the stick-slip regime, i.e., $V<V_c$.

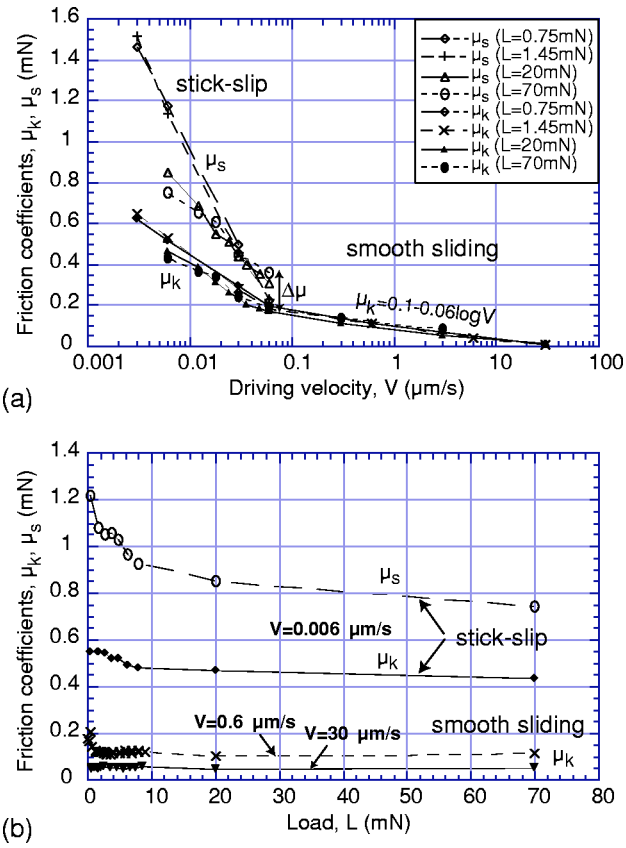

FIG. 4. (a) Friction coefficients μ_k and μ_s, as defined by Eq. (1), vs velocity V obtained at all the loads displayed in Fig. 2. (b) Friction coefficients μ_k and μ_s vs load L at the three velocities shown in Fig. 3 (values corresponding the higher loads of 20 and 70 mN have been added).

words, the friction force is not proportional to the "real" contact area of the surfaces, as is assumed in some theories of friction. We also note that there is almost no hysteresis in either curve. This manifestation of Amontons' law under Hertzian conditions at the molecular level was recently noted for thin lubricating water films [21]. In addition, whereas in the case of water the friction coefficient was independent of the sliding velocity, here we find it to fall with increasing V, although it remains constant so long as V does not change. Recently, Robbins [22] and Landman [23] performed molecular-dynamic simulations that confirmed that $F=\mu L$ at the molecular level, even at constant area A.

It is important to note that these findings and conclusions appear to apply only when there is *no adhesion* between the surfaces, i.e., when the friction is totally "load-controlled." This is the case for squalane films and water films in high salt solutions where the adhesion is zero or very small [21]. However, in the case of *highly adhesive* surfaces, the contact area is now determined by the so-called "JKR equation" [24] rather than the "Hertz equation," Eq. (3). In such cases, the contact area A and friction forces F are finite even at zero load, and there is now an additional contribution to F that is proportional to A [25]. But this situation, called the "adhesion-controlled" friction, does not pertain to the present studies with squalane where both the friction force and the contact areas vanish at $L=0$ for all values of V ($V>V_c$).

Figure 3(b) shows data for F versus L in the stick-slip regime, i.e., at $V<V_c$. The contact area A is not displayed here since it is the same as in Fig. 3(a). However the friction behavior is now different from that occurring during smooth sliding. Neither F_s nor F_k increase linearly with the load L, and both are more than an order of magnitude higher than in the smooth sliding regime (at higher velocities), and the "pseudo" friction coefficient is also 10 times larger. The friction forces were also compared to the corresponding contact areas, but no simple correlation was found between them. In addition, there was hysteresis in the measured friction forces at low loads, in contrast to the total absence of hysteresis in the case of nonadhesive sliding [Fig. 3(a)].

Figure 4(a) displays the friction coefficients μ_k and μ_s, as defined by Eq. (1), versus velocity V at all the loads displayed in Fig. 2. In the smooth sliding regime ($V>V_c$), there is an almost perfect overlap of the curves, showing that the friction coefficient μ_k follows a logarithmic law:

$$\mu_k=-C\log V \quad \text{for} \quad V>V_c, \tag{4}$$

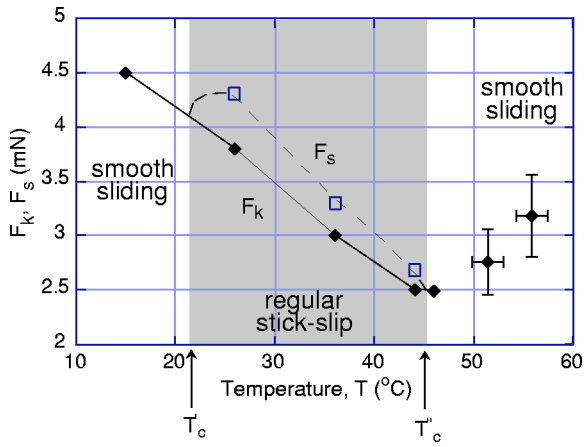

FIG. 5. Steady-state friction forces at different temperatures between 14.5 and 46 °C measured at constant load $L=18$ mN, contact diameter $2r=280$ μm, contact area $A=\pi r^2=4.5\times10^4$ μm^2, contact pressure $P=L/A=0.4$ MPa, and driving velocity $V=0.024$ μm/s (the sawtooth amplitude and frequency were kept constant at 120 μm and 0.0001 Hz, respectively). The steady-state friction shown was reached after 12 h at 26 °C, after 8 h at 36 °C, and after 3 h at 46 °C. At 15 °C, the system takes more than 20 h to reach its equilibrium state.

where $C=0.06\pm0.01$ is independent of L but depends on the temperature (see below). In the stick-slip regime ($V<V_c$), both μ_s and μ_k fall logarithmically with V, but the values for C now depend on L, decreasing as L increases. At the transition, when $V=V_c$, there is an abrupt decrease in $\Delta\mu=(\mu_k-\mu_s)$ to zero, where $\Delta\mu$ increases with L. Figure 4(b) displays μ_k and μ_s versus load L at three different velocities spanning the stick-slip and smooth sliding regimes. It better shows how the friction coefficients decrease with load in the stick-slip regime, especially at low V ($V\ll V_c$). The increasing friction with load at low velocities is likely to be due to the emergence of shear-induced adhesion between the surfaces under these conditions (see Sec. III D).

The implications of these results for understanding tribological and seismic systems are discussed in Sec. IV.

C. Effect of temperature

The friction forces shown in the previous figures were all measured at the same temperature of 26 °C. Figure 5 shows the steady-state friction forces measured at a fixed load (pressure) and sliding velocity but at different temperatures. Again, steady-state conditions were sometimes reached only after several hours of continuous (back and forth) shearing. Somewhat unexpectedly, the disappearance of stick-slip was observed both below a ''lower'' and above an ''upper'' critical temperature, T_c' and T_c'', which may be related to the recent findings of lower and upper critical *velocities* in certain boundary-lubricated systems [26]. Also, the overall friction forces decreased as the temperature was raised. The two data points with large lateral and normal error bars showed at $T>T_c''$ refer to non-steady-states, i.e., to the transient friction measured as the temperature was raised too fast for the system to have time to ''equilibrate'' and hence to accurately measure the steady-state friction force. In this regime, corresponding also to smooth sliding, the friction increases with temperature for reasons that are discussed later.

A notable feature of the friction forces described so far in Figs. 2 and 3 is that whenever there is a transition from stick-slip to smooth sliding, or vice versa, it is the kinetic friction force F_k that appears to be smoothly varying through the transition, rather than the static friction force F_s.

D. Changes in film structure and properties induced by prolonged shear

In these experiments, the surfaces were continuously visualized via the FECO interference fringes, which gave the instantaneous surface profile, contact area and thickness of the shearing junctions. More importantly, it allowed us to correlate any changes observed in the geometry of the junctions with the changing friction forces, load, velocity, temperature or sliding time. In general, as previously measured for squalane films at lower loads and room temperature [4,10], the film thickness decreased monotonically with increasing load. In our experiments, the thickness D varied monotonically from $D=2.5$ to $D=1.5$ nm as the load increased from $L=0$ to $L=70$ mN. The absence of an oscillatory force—one having multiple adhesive minima at discrete surface separations corresponding to integral layers of squalane—indicates that confined squalane is in a disordered (amorphous or glassy) state, with much interlayer entanglement [27]. However, this applies to films under pure compression. Here we find that, when *sheared*, the films can apparently be induced to undergo a phase transition.

Figure 6 shows the local sheared junction geometry during an experiment in which the temperature was changed. At 26 °C, the film thickness is fairly uniform and equal to $D=1.7-2.1$ nm over a large area (Fig. 6, top).

At 15 °C (Fig. 6, bottom), simultaneously with the disappearance of the stick-slip (Fig. 5), a second well-defined zone appears within the film of thickness $D=1.0-1.2$ nm, corresponding to approximately two layers of squalane. Within this central zone the molecules appear to have become ''shear-aligned'' into layers, as manifested by the sudden appearance of a large adhesion force: for whereas there was no measurable adhesion on separation after a normal compression (without shear) [4,10,15], there was now a large adhesion force of $F_{ad}=6$ mN, which is a typical value for the second, third, or fourth minimum of films composed of *saturated* alkanes and other small, symmetrical hydrocarbon molecules [28,29]. The appearance of the new, presumably ordered phase at 15 °C was gradual, starting or ''nucleating'' at the center (where the local pressure is highest) after 4 h of sliding, and growing radially outward as the shearing progressed over a period of 12 h until steady-state conditions were attained. It did not continue to grow when the shearing was stopped, nor did the new phase disappear when the temperature was raised back to 26 °C with the surfaces in contact. The appearance of the ordered phase was accompanied not only by an abrupt adhesion force, but also the reduction

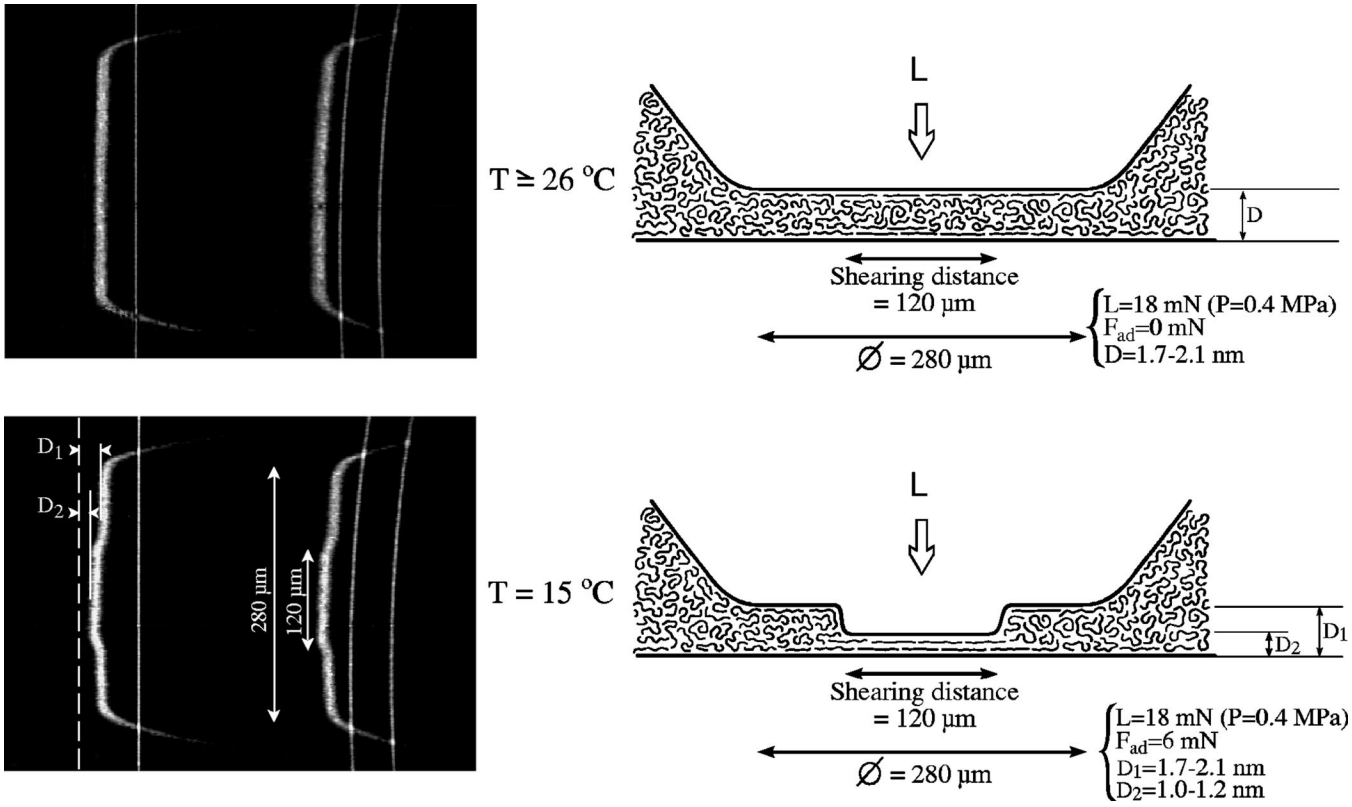

FIG. 6. Geometry of shearing junctions at 26 °C after 13 h of sliding (top), and at 15 °C after 20 h of sliding (bottom), keeping all the other experimental conditions unchanged as in Fig. 5. Left panels: FECO images of shearing junctions. Right panels: corresponding shapes of the surfaces.

and ultimate disappearance of the stick-slip friction,[4] even as the *magnitude* of the friction force itself (at least the kinetic friction force F_k) continued to increase (cf. Fig. 5). The disappearance of stick-slip may be related to the ordering of the molecules into layers, allowing for smoother sliding without the need to break entangled knots along the way. During all the measurements performed at 26 °C, applying pressure alone was never sufficient for inducing an ordering transition, and no adhesion force was ever detected, in agreement with previous results [4,10,15]. However, the low-temperature ordered state remained trapped when the temperature was raised back to 26 °C.

To clarify the effect of temperature, the same experiment was repeated without applying shear. The system did not show the effect described in Fig. 6 when it was brought, without shearing, to 15 °C (the FECO remain flat at $D = D_1$), indicating that temperature and pressure alone are not enough to induce ordering in the system, and that shearing is crucial. In addition, we note that the diameter of the thinner phase was about 120 μm, which was also the distance that the film was sheared (cf. the legend to Fig. 6) indicating an evident contribution of the shearing length to the transition. The importance of the shearing *distance* in determining tribological properties (in contrast and in addition to the shearing *time*) has been noted before [9,10]. The implications of shear-induced transitions are discussed further in Sec. IV.

E. Long-lived transient effects and slow relaxations/transitions to rest or steady-state sliding

Many important tribological phenomena reflect ''transient'' rather than ''steady-state'' or ''equilibrium'' behavior. These transient effects were therefore deemed worthy of detailed study.

1. Transition to steady-state sliding

We have already noted the very long times (hours) and long total sliding distances (millimeters) that squalane films take to reach steady-state conditions, even at temperatures well above the melting point of bulk squalane.

2. Relaxations after cessation of sliding

Under static conditions, e.g., after the cessation of sliding, long-term relaxation processes are still operating which can be measured in ''stop-start'' experiments [18,19]. In these, the hydrocarbon film is sheared at a certain velocity $V > V_c$ until smooth steady-state sliding is reached. Keeping the film under confinement, the shear is stopped for a given ''stopping'' time t_s and then resumed at the same velocity V. The evolution of the friction force is followed through the whole process. It has been reported before [4,18,19,30] that when t_s is longer than some characteristic ''latency'' time, τ_0, a peak in the friction force is usually observed when the sliding is

[4]Alternatively, as discussed in the following section, the stick-slip remained but took on a very long period.

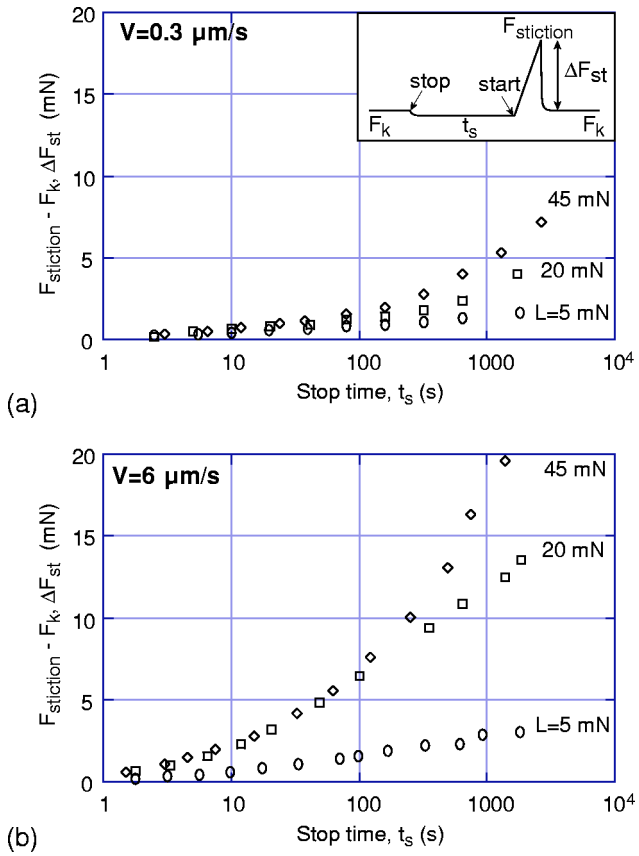

FIG. 7. Stiction spike heights ΔF_{st} as a function of stopping times t_s at different sliding speeds V and loads L, all measured at 26 °C.

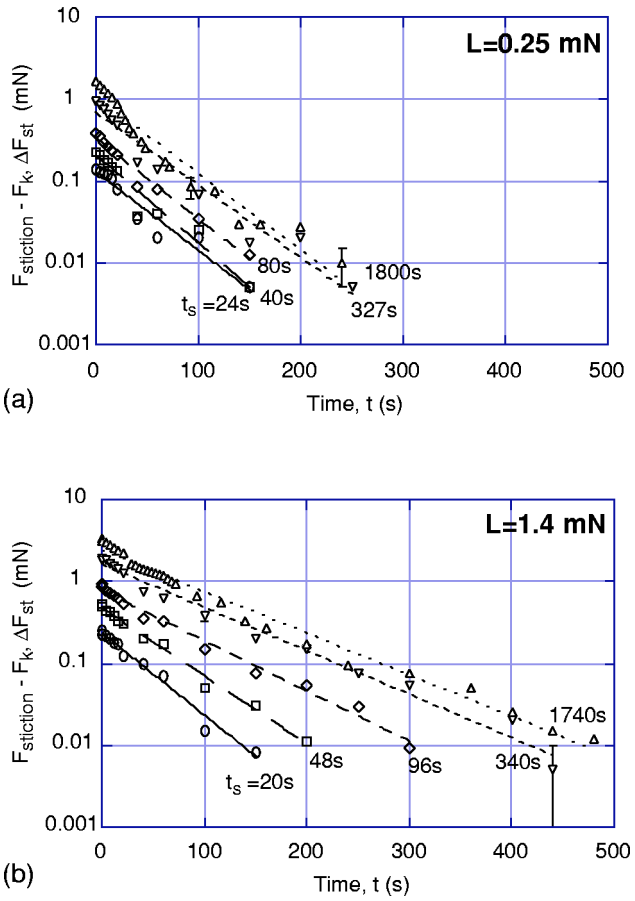

FIG. 8. Relaxation of the stiction spikes $\Delta F_{st}=F_s-F_k$ after different stopping times t_s at two different loads: (a) $L=0.25$ mN, (b) $L=1.4$ mN. All measurements were made in the smooth sliding regime ($V=0.6\ \mu$m/s$>V_c$) at $T=26$ °C.

resumed. This peak is called a ''stiction spike'' and its magnitude is defined by $\Delta F_{st}=F_{stiction}-F_k$, as shown in the inset of Fig. 7(a). In the following, we report the results of stop-start experiments performed at different sliding velocities and loads. In each case, ΔF_{st} increases with the stopping time, and shows no sign of plateauing even after 1 h. On the contrary, even the *rate* of increase continues to rise. ΔF_{st} is higher at higher shear loads, as might be expected; but it is also higher at higher sliding velocities. This is in contrast to the lower kinetic friction F_k at higher V. Part of the higher ΔF_{st} is due to the lower F_k, since this acts to increase the value of $F_{stiction}-F_k$, but most of the effect on ΔF_{st} comes from a higher $F_{stiction}$ at higher loads.

At low loads, the growth in ΔF_{st} is close to being logarithmic, as has been observed before in other tribological systems: multiple asperity contacts of rocks [31], paper [32], rough polymer surfaces [33], and fluorocarbon monolayers confined between smooth surfaces [30]. However ΔF_{st} cannot be fitted by a single logarithmic or power law function over the whole range of stopping times (and loads) studied. Interestingly, ΔF_{st} appears to extrapolate to 0 as $t_s\rightarrow 0$. Thus there is no ''latency'' time τ for squalane films, as there is for other systems that generally involve symmetrical molecules [18]. For example, Ref. [18] shows that linear saturated alkane films undergo an abrupt liquid-to-solid nucleation transition after a finite stopping time τ_0 at which point ΔF_{st} increases abruptly to some large finite value and then remains unchanged at this value with increasing t_s. The results of Fig. 7 show that after sliding has stopped, a confined film (or the surfaces themselves) takes an extremely long time to relax back to some equilibrium state. Importantly, the change in the contact area during the resting period was negligible, even under a load, so that the increased friction while the surfaces are at rest cannot be attributed to this effect.

3. Slip times during sliding

The very long sliding time or distance needed to attain steady-state sliding is but one of a number of different relaxation processes during sliding. Another is the ''slip time'' τ_{slip} for the friction force to go from F_s to F_k, for example, after a stiction spike. As shown in Fig. 8, the slip times of the stiction spikes for squalane films are of the order of seconds or minutes. These are much shorter than the hours needed to attain steady-state conditions, but still significantly longer than the natural frequency (~ 0.02 s) of the friction-force-measuring spring.[5] Thus, these times, too, are determined by some tribological property of the shearing film rather than by the inertia of the system. Figure 8 shows that the slip times

[5]This is often referred to as ''overdamped'' conditions [20].

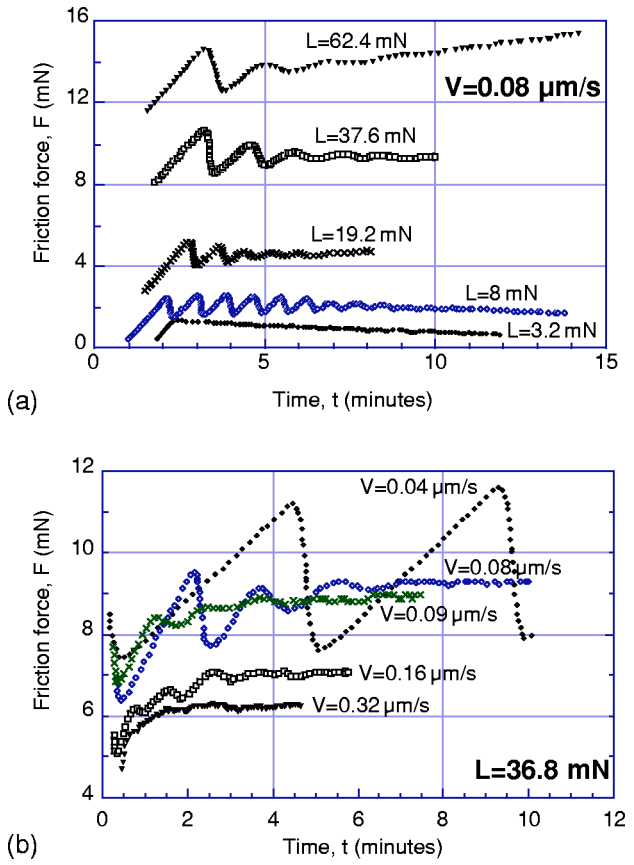

FIG. 9. (a) Transient friction forces vs time as the normal load is decreased from $L=62.4$ to 3.2 mN at constant sliding velocity of $V=0.08$ μm/s. (b) Transient friction forces vs time as the sliding velocity is increased from $V=0.04$ to 0.32 μm/s at a constant load of $L=36.8$ mN.

τ_{slip} increase with the load, but are only weakly dependent on the stopping time t_s at any given load. It also shows that the decay is roughly exponential, especially for short slip times.

4. Relaxation after a change in sliding velocity or load

Previous studies with squalane at low loads, where only smooth sliding is observed [10], found that after a change in the sliding velocity or load the friction force changed monotonically with time (or distance) until steady-state conditions were reached. This time was on the order of minutes and therefore of the same order of magnitude as the slip time τ_{slip}, described above. At the higher loads studied here, the friction acquires a stick-slip component, and the decay to steady-state sliding now involves not only the mean friction but also the stick-slip component, as shown in Fig. 9(a) for loads above 3.2 mN. Thus, initially, with increasing load, both the stick-slip amplitude $\Delta F=(F_s-F_k)$ and the mean friction force, which may be defined by $\overline{F}=1/2(F_s+F_k)$, decay with time or distance. However, at high loads or pressures, the mean friction force $\overline{F}$ increases with time, and the stick-slip takes on a more symmetrical, sinusoidal shape, in contrast to the usual shape characterized by a slow stick and fast slip. In all cases, however, the stick-slip component gradually decayed as the friction proceeded towards smooth sliding (steady state at this sliding velocity). Figure 9(b) shows the same effect but now keeping the load constant at $L=36.8$ mN while changing the sliding velocity. The friction exhibits increasingly regular stick-slip spikes as V falls below V_c (cf. Fig. 2), but near $V_c \simeq 0.06$ μm/s it is more sinusoidal and of steadily decreasing amplitude.

IV. DISCUSSION

The complexity of the results makes them difficult to summarize in one neat package. When the experimental conditions of load, speed, temperature, and time were varied over a large range, almost every conceivable type of friction force was measured—behavior that had previously been thought to belong only to particular systems. This includes not only lubricated systems, but also dry (unlubricated) surfaces, rough surfaces, surfaces undergoing wear, and, in particular, traditionally nontribological systems that include geologic and seismic phenomena. For example, it was previously thought that a particular tribological system would exhibit either a continuous or a discontinuous stick-slip to smooth sliding transition, but not both. The present results show that the same system can exhibit both, depending on the experimental or environmental conditions. An additional, related, feature of the results is the many variables to which tribological behavior can depend upon: these include the traditional variables of load (pressure) and sliding velocity (shear rate), but now also the size of the junction or the contact area, the scanning distance, the number of scans, the temperature, the mechanical (inertial) properties of the system, the sliding time, and the previous history. The effects of some of these variables will now be discussed.

Our results show that changing the load during shear can take the system into a different tribological regime, manifested by a phase change in the confined film, which changes the adhesion and friction, both quantitatively and qualitatively.[6] Large effects, again both quantitative and qualitative, were also observed by changing the temperature over a small range (from 15 to 50 °C) which is far above and well away from the *bulk* melting point of squalane of -38 °C.

The main features of the results, and those that pertain most strongly to seismic effects, are the different types of stick-slip motions observed, and their (slow) evolution with time or (large) sliding distances. By ''slow'' and ''large'' we mean in comparison to the natural vibration times of the molecules in the bulk ($\sim 10^{-11}$ s), and to the molecular length (~ 3 nm). Various transient effects and relaxation processes are evident which, for a film well above its bulk melting point, were enormously long-lived. Thus, the shearing time needed to attain steady state conditions was typically more than 10 h, and even the slip times were sometimes of the order of minutes. These times are 12–15 orders of magnitude longer than the molecular relaxation time in the bulk liquid state. On the other hand, if the relaxation processes are

[6]Shear-induced phase transitions have previously been reported only for much thicker films of liquid crystals [34].

characterized by the *distance* sheared rather than the *time* [9,10], these were typically five to six orders of magnitude larger than the length of the molecules. These values are likely to apply to the contacting asperities between two shearing rock surfaces where the states and properties of the molecules at the shearing junctions may be quite different from those in the bulk (unconfined) state; indeed, the measured slip times of seconds to minutes (cf. Fig. 9) are typical of earthquakes.

Our results show that the measured friction forces cannot be accounted for simply in terms of the increased bulk viscosity of squalane at elevated pressures. Neither can the increasing friction with contact time (Fig. 7) be explained in terms of the increasing contact area (e.g., due to creep). In both cases, non-bulk-like molecular-level changes occurring within the confined nanofilm or involving the surfaces themselves are responsible for the observed effects. Thus, the tribological behavior of confined complex liquids such as squalane between two surfaces cannot be explained in terms of their bulk properties such as their melting points, phase transition temperatures, bulk viscosity, self-diffusion coefficients, molecular relaxation times, or the bulk viscoelastic properties of the confining surfaces. Their tribological behavior appears to require a noncontinuum, non-bulk-like approach that considers the dynamic (nonequilibrium) processes going on at the molecular level. Layering of squalane has been previously observed on either a single solid substrate [35] or confined between a HOPG surface and a silicon tip of an AFM [36]; however, our results provide the first experimental evidence, to our knowledge, of molecular layering of a highly *anisotropic* hydrocarbon liquid under such high conditions of confinement (nanometer-thick film over an area of thousands of μm^2) and shear. They confirm grand canonical ensemble molecular-dynamics simulations by Gao and co-workers [27] who predicted layering or out-of-plane ordering for squalanes but with no in-plane ordering (as found for linear, saturated *n*-alkanes) due to a high degree of interlayer interdigitation. These computer simulations were performed for surfaces under confinement only, i.e., without shear. Apparently, under shear, these interlayer interdigitations become undone, resulting in a more ordered, layered film, exhibiting smooth sliding and significant adhesion. The smooth sliding is probably due to the ease with which the now well-aligned layers can slip past each other without the need to continually pluck out interdigitated segments, while the adhesion is as expected across layered films but which was not previously seen across unsheared squalane films [4,10,15]. It is also interesting that the authors of Ref. [36] measured layering of squalane on a HOPG surface but could not repeat it on a mica surface. Since their measurements were carried out in air, we believe that the ''absence'' of an oscillatory force profile on mica is due to capillary forces induced by a water meniscus formed between the AFM tip and the (highly hydrophilic) mica; such forces usually induce a very high adhesion (such as the one measured by the authors) that can easily hide the ''shallow'' oscillations of the profile, rather than being a consequence of the structure of mica (since in this study we observe squalane layering on mica).

Some recent theories of friction and lubrication have recognized that a molecular-level description, rather than a continuum or mean-field approach, is called for. These involve molecular-dynamics computer simulations [8], analytic theories [37], and rate-and-state models [20,38] that are more phenomenological and where the connection between the (macroscopic) variables in the equations and what happens at the molecular level is not always clear. Another approach has been recently proposed, based on constitutive equations describing molecular rearrangements in structural systems ranging from glasses to granular materials [39]. This approach relies on the shear transformation zone theory, originally introduced to describe elastoplastic transitions in amorphous solids, in which macroscopic deformation results from local free-volume activated rearrangements at a mesoscopic scale. The STZ theory can be supplemented with the dynamics of the free volume (rather than considering the free volume as a simple parameter) to permit one to describe most of the features observed here as well as in other systems, both microscopic and macroscopic [40]: boundary lubricant layers, fluid lubricants, dry friction, rocks, paper, and rough polymer surfaces [30–33]. Both the STZ and analytic theories [37,40,41] predict a logarithmic decay of the friction force in the smooth sliding regime (indicative of continued ''shear thinning''), regular and/or chaotic stick-slip, both continuous and discontinuous stick-slip to smooth sliding transitions, and a roughly logarithmic growth of ΔF_{st} with stopping time. However, no theory at the moment takes into account all the experimental variables, such as the pressure and the temperature.

V. CONCLUSIONS

This study shows that the same tribological system can exhibit either a continuous or a discontinuous stick-slip to smooth steady-state sliding transition depending on the experimental or environmental conditions, as well as exhibit very long transient effects when the experimental parameters are changed. The system investigated also reveals both upper and lower critical transition temperatures, where the lower critical temperature is associated with the shear-induced ordering of the trapped molecules into layers between the two shearing surfaces. The system exhibited both short and very long relaxation times and/or distances compared to systems lubricated with simple spherical or linear-chained molecules, and displays many characteristics of rough, unlubricated, plastically deformable, and multiple-asperity systems. These results suggest the existence of a broad spectrum of liquidlike, solidlike, or glassy-amorphous relaxation processes in single asperity atomically smooth films that have previously been associated with different types of systems.

ACKNOWLEDGMENTS

The authors thank Dr. Anaël Lemaître for many useful discussions. This work was funded by the W. M. Keck Foundation, the Swiss National Science Foundation, and partially supported by the MRSEC Program of the U.S. National Science Foundation under Grant No. DMR00-80034.

[1] E. Rabinowicz, *Friction and Wear of Materials*, 2nd ed. (Wiley, New York, 1995).
[2] B. N. J. Persson, *Sliding Friction* (Springer-Verlag, Berlin, 1998).
[3] M. Ruths, A. D. Berman, and J. N. Israelachvili, in *Handbook of Nanotechnology*, edited by B. Bhushan (Springer-Verlag, Berlin, in press).
[4] C. Drummond and J. N. Israelachvili, Phys. Rev. E **63**, 041506 (2001).
[5] S. Granick, Science **253**, 1374 (1991).
[6] R. W. Carpick and M. Salmeron, Chem. Rev. (Washington, D.C.) **97**, 1163 (1997), and references therein.
[7] J.-M. Georges *et al.*, J. Phys. II **6**, 57 (1996); H. A. Spikes, in *Fundamentals of Tribology and Bridging the Gap between the Macro- and Micro/Nanoscales*, edited by B. Bhushan (Kluwer, Dordrecht, 2001), Vol. 10, p. 663; E. Kumacheva and J. Klein, J. Chem. Phys. **108**, 7010 (1998).
[8] P. A. Thompson, M. O. Robbins, and G. Grest, Isr. J. Chem. **35**, 93 (1995); J. Gao, W. D. Luedtke, and U. Landman, J. Phys. Chem. B **102**, 5033 (1998); Tribol. Lett. **9**, 3 (2000).
[9] M. Heuberger, G. Luengo, and J. N. Israelachvili, J. Phys. Chem. B **103**, 10127 (1999); G. Luengo, M. Heuberger, and J. N. Israelachvili, *ibid.* **104**, 7944 (2000).
[10] C. Drummond and J. N. Israelachvili, Macromolecules **33**, 4910 (2000).
[11] A. Dhinogwala, L. Cai, and S. Granick, Langmuir **12**, 4537 (1996).
[12] J. N. Israelachvili and G. E. Adams, J. Chem. Soc., Faraday Trans. 1 **74**, 975 (1978); M. Homola, J. N. Israelachvili, M. L. Gee, and P. M. McGuiggan, J. Tribol. **111**, 675 (1989).
[13] G. Luengo, F. J. Schmitt, R. Hill, and J. N. Israelachvili, Macromolecules **30**, 2482 (1997).
[14] J. N. Israelachvili, J. Colloid Interface Sci. **44**, 259 (1973); M. Heuberger, G. Luengo, and J. N. Israelachvili, Langmuir **13**, 3839 (1997).
[15] A. L. Demirel and S. Granick, Phys. Rev. Lett. **77**, 4330 (1996).
[16] H. Hertz, J. Reine Angew. Math. **92**, 156 (1882) [for English translation see *Miscellaneous Papers by H. Hertz*, edited by Jones and Schott (Macmillan, London, 1896)].
[17] J. Israelachvili, P. McGuiggan, M. Gee, A. Homola, M. Robbins, and P. Thompson, J. Phys.: Condens. Matter **2**, SA89 (1990).
[18] H. Yoshizawa and J. N. Israelachvili, J. Phys. Chem. **97**, 11 300 (1993).
[19] H. Yoshizawa, Y.-L. Chen, and J. N. Israelachvili, Wear **168**, 161 (1993).
[20] J. M. Carlson and A. Batista, Phys. Rev. E **53**, 4153 (1996).
[21] A. Berman, C. Drummond, and J. N. Israelachvili, Tribol. Lett. **4**, 95 (1998).
[22] G. He and M. O. Robbins, Tribol. Lett. **10**, 7 (2001); M. H. Muser, L. Wenning, and M. O. Robbins, Phys. Rev. Lett. **86**, 1295 (2001).
[23] J. Gao, W. D. Luedtke, and U. Landman (unpublished results).
[24] K. L. Johnson, K. Kendall, and A. D. Roberts, Proc. R. Soc. London, Ser. A **324**, 301 (1971).
[25] J. N. Israelachvili, in *Fundamentals of Friction: Macroscopic and Microscopic Processes*, edited by I. L. Singer and H. M. Pollock (Kluwer, Dordrecht, 1992), Vol. 220, p. 351.
[26] C. Drummond, J. Elezgaray, and P. Richetti, Europhys. Lett. **58**, 503 (2002).
[27] J. Gao, W. D. Luedtke, and U. Landman, J. Phys. Chem. B **106**, 4309 (1997); Phys. Rev. Lett. **79**, 705 (1997).
[28] J. N. Israelachvili, *Intermolecular and Surface Forces*, 2nd ed. (Academic Press, New York, 1992), Chap. 13, and references therein.
[29] J. Gao, W. D. Luedtke, and U. Landman, J. Phys. Chem. B **101**, 4013 (1997).
[30] S. Yamada and J. N. Israelachvili, J. Phys. Chem. B **102**, 234 (1998).
[31] J. H. Dieterich, J. Geophys. Res. B **84**(B5), 2161 (1979); J. R. Rice and A. L. Ruina, J. Appl. Mech. **50**, 343 (1983).
[32] T. Baumberger, F. Heslot, and B. Perrin, Nature (London) **367**, 544 (1994); F. Heslot, T. Baumberger, B. Perrin, B. Caroli, and C. Caroli, Phys. Rev. E **49**, 4973 (1994).
[33] P. Berthoud, T. Baumberger, C. G'Sell, and J.-M. Hiver, Phys. Rev. B **59**, 14 313 (1999).
[34] Y. Golan, A. Martin-Herranz, Y. Li, C. R. Safinya, and J. N. Israelachvili, Phys. Rev. Lett. **86**, 1263 (2001).
[35] S. Bardon *et al.*, Faraday Discuss. **104**, 307 (1996); C. Mathew Mate and B. Marchon, Phys. Rev. Lett. **85**, 3902 (2000).
[36] R. Lim and S. J. O'Shea, Phys. Rev. Lett. **88**, 246101 (2002).
[37] A. E. Filippov, J. Klafter, and M. Urbakh, Phys. Rev. Lett. **87**, 275506 (2001); J. Chem. Phys. **116**, 6871 (2002).
[38] A. Ruina, J. Geophys. Res. B **88**, 10 359 (1983).
[39] M. L. Falk and J. S. Langer, Phys. Rev. E **57**, 7192 (1998); MRS Bull. **25**, 40 (2000).
[40] A. Lemaître, Phys. Rev. Lett. **89**, 064303 (2002); **89**, 195503 (2002).
[41] A. Lemaître and J. M. Carlson (unpublished).